The Journal of Immunology



# The CXC Chemokine Murine Monokine Induced by IFN- γ (CXC Chemokine Ligand 9) Is Made by APCs, Targets Lymphocytes Including Activated B Cells, and Supports Antibody Responses to a Bacterial Pathogen In Vivo

Matthew K. Park, Doron Amichay, Paul Love, Elizabeth Wick, Fang Liao, Alex Grinberg, Ronald L. Rabin, Hongwei H. Zhang, Senkuta Gebeyehu, Timothy M. Wright, Akiko Iwasaki, Youmin Weng, Julie A. DeMartino, Karen L. Elkins and Joshua M. Farber

*J Immunol* 2002; 169:1433-1443; ;
doi: 10.4049/jimmunol.169.3.1433
http://www.jimmunol.org/content/169/3/1433



*The Journal of Immunology* is published twice each month by
The American Association of Immunologists, Inc.,
1451 Rockville Pike, Suite 650, Rockville, MD 20852

Print ISSN: 0022-1767 Online ISSN: 1550-6606.

# The CXC Chemokine Murine Monokine Induced by IFN-γ (CXC Chemokine Ligand 9) Is Made by APCs, Targets Lymphocytes Including Activated B Cells, and Supports Antibody Responses to a Bacterial Pathogen In Vivo

**Matthew K. Park,* Doron Amichay,* Paul Love,‡ Elizabeth Wick,* Fang Liao,* Alex Grinberg,‡ Ronald L. Rabin,* Hongwei H. Zhang,* Senkuta Gebeyehu,* Timothy M. Wright,¶ Akiko Iwasaki,† Youmin Weng,‖ Julie A. DeMartino,‖ Karen L. Elkins,§ and Joshua M. Farber[1]***

**Monokine induced by IFN-γ (Mig; CXC chemokine ligand 9) is an IFN-γ-inducible CXC chemokine that signals through the receptor CXCR3 and is known to function as a chemotactic factor for human T cells, particularly following T cell activation. The *mig* gene can be induced in multiple cell types and organs, and Mig has been shown to contribute to T cell infiltration into immune/inflammatory reactions in peripheral tissues in mice. We have investigated the expression and activities of Mig and CXCR3 in mouse cells and the role of Mig in models of host defense in mice. Murine (Mu)Mig functioned as a chemotactic factor for resting memory and activated T cells, both $CD4^+$ and $CD8^+$, and responsiveness to MuMig correlated with surface expression of MuCXCR3. Using $mig^{-/-}$ mice, we found that MuMig was not necessary for survival after infections with a number of intracellular pathogens. Surprisingly, however, we found that $mig^{-/-}$ mice showed reductions of 50–75% in Abs produced against the intracellular bacterium *Francisella tularensis* live vaccine strain. Furthermore, we found that MuMig induced both calcium signals and chemotaxis in activated B cells, and that B cell activation induced expression of MuCXCR3. In addition, IFN-γ induced the expression of *mumig* in APCs, including $CD8\alpha^+$ and $CD8\alpha^-$ dendritic cells. Together, our data suggest that Mig and CXCR3 may be important not only to recruit T cells to peripheral inflammatory sites, but also in some cases to maximize interactions among activated T cells, B cells, and dendritic cells within lymphoid organs to provide optimal humoral responses to pathogens. *The Journal of Immunology,* 2002, 169: 1433–1443.**

As the numbers of members within the families of chemokines and their receptors have grown, so too has the interest in the biological roles of these proteins, which are increasingly appreciated to be critical for the development, anatomic organization, and effective protective responses of the immune system (for reviews see Refs. 1 and 2). Much recent work has focused on understanding the distinctive roles of individual chemokine/receptor groups in lymphocyte biology. This work has revealed that some ligands/receptors are important for trafficking during homeostasis, such as secondary lymphoid tissue chemokine (CC chemokine ligand (CCL)[2]21)/CCR7, EBV-induced receptor ligand chemokine (CCL19)/CCR7, and B lymphocyte chemoattractant (CXC chemokine ligand (CXCL)13)/CXCR5, which function in the T cell regions and follicles, respectively, of secondary lymphoid organs, while other ligands/receptors are associated with inflammatory responses at diverse tissue sites (for review see Ref. 3).

Monokine induced by IFN-γ (Mig; CXCL9) is one of the three non-ELR (lacking a GluLeuArg motif in the N-terminal region) CXC chemokines that are associated with inflammatory reactions (for review see Ref. 4). These three chemokines target lymphocytes and signal through the receptor CXCR3. Mouse and human *mig* were described as genes induced specifically by IFN-γ (5, 6). The human (Hu)Mig protein was found to be a chemoattractant for activated, tumor-infiltrating lymphocytes (7) and for $CD4^+$ and $CD8^+$ peripheral blood T cells (8). In humans, Mig has been associated with T cell infiltration in inflammatory diseases of the skin (9, 10), joints (11), and CNS (12, 13) and in malignancy (14). In mouse models, Mig is highly induced in an IFN-γ-dependent fashion during cell-mediated responses to pathogens (15) and has been shown to be active in antiviral defense (16, 17) and in mediating the rejection of tumors (18, 19) and allografts (20, 21).

CXCR3 is the only known receptor for Mig. Mig shares CXCR3 with IFN-γ-inducible protein-10 (IP-10; CXCL10) (7, 22) and

*Inflammation Biology Section and †Immune Cell Interaction Unit, Laboratory of Clinical Investigation, National Institute of Allergy and Infectious Diseases, ‡Laboratory of Mammalian Genes and Development, National Institute of Child Health and Human Development, National Institutes of Health, and §Division of Bacterial, Parasitic, and Allergenic Products, Center for Biologics Evaluation and Research, Food and Drug Administration, Bethesda, MD 20892; ¶Experimental Medicine and Inflammation Pharmacology, Pfizer Global R&D, Ann Arbor, MI 48105; and ‖Department of Immunology Research, Merck Research Laboratories, Rahway, NJ 07065

Received for publication September 17, 2001. Accepted for publication May 30, 2002.

The costs of publication of this article were defrayed in part by the payment of page charges. This article must therefore be hereby marked *advertisement* in accordance with 18 U.S.C. Section 1734 solely to indicate this fact.

[1] Address correspondence and reprint requests to Dr. Joshua M. Farber, Laboratory of Clinical Investigation, National Institute of Allergy and Infectious Diseases, National Institutes of Health, Building 10, Room 11N228, MSC-1888, Bethesda, MD 20892-1888. E-mail address: joshua_farber@nih.gov

[2] Abbreviations used in this paper: CCL, CC chemokine ligand; CRG, cytokine-responsive gene; CXCL, CXC chemokine ligand; ES, embryonic stem; Hu, human; i.d., intradermal(ly); IP-10, IFN-γ-inducible protein-10; I-TAC, IFN-inducible T cell α-chemoattractant; PGK, phosphoglycerate kinase; LVS, live vaccine strain; Mig, monokine induced by IFN-γ; MIP, macrophage-inflammatory protein; Mu, murine; SSS-III, type III pneumococcal polysaccharide; CD40L, CD40 ligand; TNP, trinitrophenyl; KLH, keyhole limpet hemocyanin; GFP, green fluorescent protein.



0022-1767/02/$02.00

IFN-inducible T cell α-chemoattractant (I-TAC; CXCL11) (23), and CXCR3 is expressed on subsets of human peripheral blood T, B, and NK cells (Ref. 24 and reviewed in Ref. 25). The human CXCR3 is expressed on naive and memory $CD8^+$ T cells and on memory $CD4^+$ T cells and can be induced on all T cell subsets within the first few days after activation (8). CXCR3 is induced to higher levels on human Th1 as compared with Th2 cell lines (26) and is found on all Th1 memory cells in peripheral blood (27). Experiments with CXCR3 knockout mice have shown that CXCR3 contributes to T cell proliferation in vitro in a MLR, and to acute rejection of heart allografts, with transplants in the knockout mice showing diminished inflammation and prolonged survival (28).

Together the data suggest that the primary role of CXCR3 and its ligands is in the recruitment of effector T cells, and among Th cells the Th1 subset in particular, to sites of peripheral inflammation during a type 1 immune response, possibly with a direct role in T cell activation. Nonetheless, there has been no systematic examination of the activities of murine (Mu)Mig and the expression and activities of CXCR3 on mouse cells, and experiments on the roles of this ligand/receptor pair in vivo in mice, as described above, have been limited. In the data presented in this work we demonstrate that MuMig targets both T and B cells, which can express CXCR3, and that the murine *mig* gene can be produced by all classes of APCs. Furthermore, we show that MuMig contributes to the optimal humoral response to a bacterial pathogen. Together, our observations suggest that roles for Mig, and by implication perhaps other inflammatory chemokines, are not limited to recruiting cells at peripheral sites of inflammation but may extend to maximizing cell-cell interactions and immune responses within lymphoid organs.

## Materials and Methods

### *Mice*

C57BL/6 mice were purchased from the Division of Cancer Therapy of the National Cancer Institute (Frederick, MD); 129/Sv mice were obtained from the Division of Cancer Therapy of the National Cancer Institute and bred at the National Institutes of Health (Bethesda, MD); and C57BL/6J-TCR$\beta^-$TCR$\delta^-$ mice were purchased from The Jackson Laboratory (Bar Harbor, ME). The $mig^{-/-}$ mice were derived from two colonies of gene-targeted embryonic stem (ES) cells and used in the 129/Sv, (129/Sv × C57BL/6)$F_2$, and C57BL/6 backgrounds (see below). All mice ranged between 8 and 20 wk old and were housed in sterile cages under pathogen-free conditions. Animal protocols were approved by the Animal Care and Use Committees of the National Institute of Allergy and Infectious Diseases (National Institutes of Health) and the Center for Biologics Evaluation and Research (Food and Drug Administration, Bethesda, MD).

### *Preparing, culturing, and activating mouse leukocytes*

RPMI 1640 (Life Technologies, Gaithersburg, MD) for culturing mouse lymphocytes contained 10% FBS, 55 μM 2-ME, 1 mM pyruvate, 2 mM glutamine, 100 μM nonessential amino acids, and 100 U/ml penicillin-streptomycin. Cell staining for analyzing and sorting lymphocytes was done with the following Abs: for CD4, clone GK1.5 conjugated to allophycocyanin (Leinco Technologies, Ballwin, MO) or clone H129.19 conjugated to FITC or Cy5-PE (BD PharMingen, San Diego, CA); for CD8α, clone 53-6.7 conjugated to FITC, PE, or allophycocyanin; for CD45R/B220, clone RA3-6B2, conjugated to FITC, PE, or allophycocyanin; for CD11b, clone M1/70 conjugated to FITC or allophycocyanin; for CD11c, clone HL3 conjugated to FITC; for NK1.1, clone PK136 conjugated to FITC; for CD62L, clone MEL-14 conjugated to FITC; and for CD44, clone IM7 conjugated to FITC, PE, or Cy5-PE (all from BD PharMingen).

Assays for T cell chemotaxis and staining of T cells for flow cytometry used splenocyte preparations from C57BL/6 mice. For activation of T cells in the splenocyte population, $10^6$ splenocytes per milliliter were cultured in 24-well plates that had been coated with 10 μg/ml anti-CD3 (145-2C11; BD PharMingen). Cells were harvested on day 3 or 4. For studying CXCR3 expression on $CD8^+$ T cells, splenocytes were first enriched for $CD8^+$ T cells using murine T cell CD8 subset columns (R&D Systems, Minneapolis, MN) and then sorted into $CD8^+CXCR3^-$ and $CD8^+CXCR3^+$ populations that were $CD4^-CD11b^-CD11c^-B220^-NK1.1^-$ using a FACStar or FACSVantage cell sorter (BD Immunocytometry Systems, San Jose, CA). These and other populations of sorted cells were always >95% pure. The $CD8^+$ T cells were plated at $1 \times 10^6$ cells/ml in 96-well plates coated with anti-CD3 (10 μg/ml) and containing anti-CD28 (10 μg/ml, clone 37.51; BD PharMingen) and cultured for 4 days.

For purifying T cells as sources of RNA for RT-PCR, splenocytes from C57BL/6 mice were passed over a T cell enrichment column according to the manufacturer's protocol (R&D Systems) and $CD4^+$ and $CD8^+$ lymphocytes were purified by sorting on a FACStar cell sorter for cells that were $CD4^+CD8\alpha^-CD45R/B220^-CD11b^-$ and $CD8\alpha^+CD4^-CD45R/B220^-CD11b^-$, respectively. For activating these sorted T cells, $5 \times 10^6$ cells/ml were incubated for 18 h in 96-well flat-bottom plates with anti-CD3 and anti-CD28 as above.

To isolate B cells for staining, calcium flux, chemotaxis, and preparing RNA for Northern analysis, splenocytes from C57BL/6J-TCR$\beta^-$TCR$\delta^-$ mice were plated onto polystyrene dishes at $10^7$ cells/ml in DMEM/2% FBS for 30 min at 37°C and the nonadherent cells were harvested, which were 90% B cells as determined by B220 staining. For purifying B cells as sources of RNA for RT-PCR, splenocytes were harvested from C57BL/6J-TCR$\beta^-$TCR$\delta^-$ mice and $CD45R/B220^+CD11b^-$ cells were isolated by cell sorting as above. For activation for staining for flow cytometry, calcium flux, and chemotaxis, B cells were plated at $10^6$ cells/ml onto irradiated, CD40 ligand (CD40L)-expressing fibroblasts (gift from B. Kelsall, National Institute of Allergy and Infectious Diseases, National Institutes of Health) in six-well plates in RPMI medium as above plus 5 ng/ml murine rIL-4 (BioSource International, Rockville, MD) and 10 μg/ml goat $F(ab')_2$ anti-mouse IgM (Caltag Laboratories, Burlingame, CA, or ICN Pharmaceuticals, Aurora, OH). After 3 days, 50% fresh medium was added and cells were harvested at day 5. For activating sorted B cells as a source of RNA, $5 \times 10^6$ cells/ml were incubated for 18 h in 96-well flat-bottom plates with 10 μg/ml goat $F(ab')_2$ anti-mouse IgM (ICN Pharmaceuticals).

Enriched populations of neutrophils and macrophages were obtained at 3 or 72 h, respectively, after i.p. injection of thioglycolate. Cells were >90% neutrophils or macrophages as determined by microscopic analysis of cytospin preparations stained with Hema 3 (Biomedical Science, Swedesboro, NJ). $CD8^+$ and $CD8^-$ dendritic cells were isolated from spleens of 6- to 10-wk-old BALB/c mice by cell sorting as described (29).

### *Measurements of chemotaxis*

Assays for chemotaxis of T and B cells used either ChemoTx 96-well disposable chemotaxis plates (NeuroProbe, Cabin John, MD) or Transwell plates (Costar, Cambridge, MA). For activated lymphocytes, dead cells were removed using Ficoll-Paque Plus (Amersham Pharmacia Biotech, Uppsala, Sweden) before the assay. The ChemoTx 96-well plates contained 6-mm diameter, 5-μm pore size, polyvinylpyrrolidone-free polycarbonate membranes and were used according to the manufacturer's protocol. After incubation at 37°C for 3 h, cells from 32 lower wells were pooled, counted, stained, and analyzed as appropriate for expression of CD4, CD8α, or CD45R/B220. Assays using Transwell plates were done as described (30) using membranes with 5-μm pores and $10^6$ cells per well. Assays for chemotaxis of neutrophils and macrophages were done using polyvinylpyrrolidone-free polycarbonate membranes with 3- or 8-μm pores, respectively, in a 48-well microchemotaxis chamber (NeuroProbe). Five randomly selected fields were chosen to count cells at a ×1000 magnification. rMuMig was obtained from BD PharMingen and rHuI-TAC was obtained from PeproTech (Rocky Hill, NJ).

### *Detecting murine CXCR3 surface expression*

To generate the anti-CXCR3 Ab, rabbits were immunized with a peptide-containing sequence from the N-terminal region, YLEVSERQVLDASD FAFOrnC, conjugated to bovine thyroglobulin. Antisera were affinity purified by BioExpress Cell Culture Services (West Lebanon, NH) using peptide coupled to Sulfo-Link gel (Pierce, Rockford, IL). For surface staining for CXCR3, 0.3 mg/ml anti-CXCR3 Ab or rabbit IgG was preincubated with or without 0.5 mg/ml immunizing peptide for 30 min at room temperature, and cells were stained with 30 μg/ml of the pretreated Abs. Following incubation of cells and primary Abs for 1 h at 4°C, biotinylated goat $F(ab')_2$ anti-rabbit Ig (H and L chains; Caltag Laboratories) was added, followed by streptavidin-PE (BD PharMingen) before analysis by flow cytometry.

We isolated a mouse CXCR3 cDNA by screening a mouse splenocyte cDNA library in lambda HybriZAP (Stratagene, La Jolla, CA) kindly provided by L. Zhang and M. Lenardo (National Institute of Allergy and Infectious Diseases, National Institutes of Health), using a coding region

probe obtained from a genomic clone of the human CXCR3 kindly provided by P. Murphy (National Institute of Allergy and Infectious Diseases, National Institutes of Health). cDNAs were isolated that matched the sequences subsequently published for mouse CXCR3 (31). To determine the specificity of the anti-CXCR3 Ab, Jurkat-TAg cells (derived as described (32) and kindly provided by L. Samelson, National Cancer Institute, National Institutes of Health) were transfected with 40 $\mu$g of either pCEFL (33) or pCEFL into which the mouse CXCR3 cDNA had been inserted, plus 25 $\mu$g of pEGFP-F encoding a farnesylated green fluorescent protein (GFP; Clontech Laboratories, Palo Alto, CA) as described (34) to identify cells expressing the transfected genes. The cotransfected cells expressing enhanced farnesylated GFP (but not the enhanced GFP-negative cells) stained with the anti-MuCXCR3 Ab, but not with control rabbit IgG, and the Ab staining was blocked by preincubation with the immunizing peptide. Similarly, a transfected RBL-1 cell line expressing MuCXCR3 showed staining with the anti-MuCXCR3 Ab that was blocked by the immunizing peptide, but not by an irrelevant peptide corresponding to N-terminal residues from MuCCR6 (data not shown).

### *Targeting of the mouse* mig *gene*

Choices of fragments to use for homologous recombination and as probes in targeting the *mig* gene were based on 7.1 kb of sequence obtained from clones from an EMBL-3, C3H mouse genomic library kindly provided by R. Reeves (Johns Hopkins University) (J. M. Farber and T. M. Wright, unpublished data). To isolate DNA fragments for gene targeting, recombinant bacteriophage P1 clones containing the *mig* gene from a 129 mouse were obtained from Genome Systems (St. Louis, MO) after screening by PCR using primers from the gene's fourth exon. DNA was isolated from the P1 clone for gene targeting that included a 5′ *Bsm*I fragment of 1802 bp, containing exon 1 and 22 bp of exon 2, and a 3′ *Eco*RI/*Bsm*I fragment of 2752 bp containing exons 3 and 4 (see Fig. 3).

Adapters were used to ligate the 5′ *Bsm*I fragment and the 3′ *Eco*RI/*Bsm*I fragment into the unique *Xho*I and *Eco*RI sites, respectively, of pPNT (35), which contains the neomycin resistance gene (*neo*) and the *hsv-thymidine kinase* gene, each driven by the phosphoglycerate kinase (PGK) promoter. pPNT-*mumig* was linearized using the unique *Not*I site. Transfection of J1 ES cells (passage 12) and selection with G418 and ganciclovir were done as described (36). DNAs from 191 G418/ganciclovir-resistant colonies were digested with *Pst*I and screened by Southern analysis using as probe a 450-bp fragment from the flanking region of the *mig* gene outside of the 5′ *Bsm*I *mig* fragment used in pPNT-*mumig* (see Fig. 3). DNAs from 12 ES cell colonies yielded a *Pst*I fragment of ~7 kb as predicted in the event of homologous recombination. These ES clones were analyzed with additional probes to ensure that the structure of the recombinant locus was as predicted. All but one of the ES clones were shown to have a single copy of the inserted *neo* gene.

### *Producing* mig$^{-/-}$ *mice and breeding mice for experiments*

Cells from two ES clones (numbers 17 and 63) gave chimeric progeny (as judged by coat color) after injection into C57BL/6 blastocysts as described (36), and offspring of matings between C57BL/6 females and male chimeras (lines 17 and 63) or 129/Sv females and male chimeras (line 63) showed transmission of the recombined locus as judged by Southern blotting of *Pst*I-digested DNA as described above and/or by a PCR-based assay, the details of which are available on request.

Offspring of chimeras derived from ES clone 17 were intercrossed to produce *mig*$^{-/-}$ and *mig*$^{+/+}$ (129/Sv × C57BL/6)$F_2$ mice. For some experiments, the *mig*$^{-/-}$ and *mig*$^{+/+}$ (129/Sv × C57BL/6)$F_2$ mice were offspring of *mig*$^{-/-}$ × *mig*$^{-/-}$ or *mig*$^{+/+}$ × *mig*$^{+/+}$ matings. In these cases, all the *mig* homozygous breeders were offspring from (129/Sv × C57BL/6)$F_1$ mice, making them genetically equivalent to siblings. For some experiments, the *mig*$^{-/-}$ and *mig*$^{+/+}$ (129/Sv × C57BL/6)$F_2$ mice were offspring of *mig*$^{+/-}$ × *mig*$^{+/-}$ matings. In these cases, the *mig*$^{+/-}$ breeders were offspring from (129/Sv × C57BL/6)$F_1$ mice, making them genetically equivalent to siblings, or the direct offspring of these mice, and the *mig*$^{-/-}$ and *mig*$^{+/+}$ mice used in experiments shared parents insofar as was practical. In later experiments, mice derived after backcrossing six generations into C57BL/6 mice were intercrossed to generate *mig*$^{-/-}$ mice, which were used in experiments with control C57BL/6 mice from the Division of Cancer Therapy of the National Cancer Institute. Some experiments (data not shown) used mice derived from ES clone 63 that were crossed with 129/Sv mice before intercrossing to generate *mig*$^{-/-}$ mice (from *mig*$^{-/-}$ × *mig*$^{-/-}$ matings) that were used with wild-type, control 129/Sv mice bred in our facility.

### *Analyzing* mig$^{-/-}$ *and* mig$^{+/+}$ *mice for Mig protein*

Analysis of production of MuMig protein in the liver by Western blot was done as described (15). MuMig protein was detected using 10 $\mu$g/ml rabbit anti-MuMig Ab 5170 that had been raised against the full-length, rMuMig (purified in our laboratory from supernatants from BTI-TN-5B1-4 *Trichoplusia ni* cells infected with recombinant baculovirus) and affinity purified using rMuMig (PeproTech) that had been coupled to Affigel 10 (Bio-Rad) according to the manufacturer's protocol. Bound Ab was detected on the blot using 0.16 $\mu$g/ml HRP-conjugated goat anti-rabbit IgG (Santa Cruz Biotechnology, Santa Cruz, CA) and SuperSignal chemiluminescent substrate (Pierce) according to the manufacturer's protocol.

### *Infections and Ab responses with* Francisella tularensis *LVS in* mig$^{-/-}$ *and* mig$^{+/+}$ *mice*

After obtaining preimmunization serum samples, male *mig*$^{-/-}$ and *mig*$^{+/+}$ mice were infected intradermally (i.d.) at the base of the tail with $10^4$–$10^7$ CFU *F. tularensis* live vaccine strain (LVS). Sera were obtained from weekly bleeds, stored at −20°C, and batch run for anti-*F. tularensis* LVS titers as described previously (37), using an ELISA with isotype-specific detection reagents from Southern Biotechnology Associates (Birmingham, AL) and plates coated with live *F. tularensis* LVS bacteria. End point titer was defined as the lowest dilution of serum that gave an $OD_{405}$ value >0.050 OD units and that was also 2 SDs of the mean greater than the OD value of the matched dilution of normal, pre-bleed mouse serum.

### *Thymus-dependent and thymus-independent Ab responses in* mig$^{-/-}$ *and* mig$^{+/+}$ *mice*

For determining thymus-dependent Ab responses, *mig*$^{-/-}$ and *mig*$^{+/+}$ (129/Sv × C57BL/6)$F_2$ littermates were injected i.p. with 200 $\mu$g of (2,4,6)trinitrophenyl (TNP)-keyhole limpet hemocyanin (KLH) in solution without adjuvant (Biosearch Technologies, Novato, CA) and serum was collected at weekly intervals through wk 4. Ab responses were measured using ELISA with TNP-BSA as described (37). For determining thymus-independent Ab responses, *mig*$^{-/-}$ and *mig*$^{+/+}$ (129/Sv × C57BL/6)$F_2$ littermates were injected with either 1 $\mu$g of *Escherichia coli* LPS serotype 055:B5 (Sigma-Aldrich, St. Louis, MO) i.p. or 0.5 $\mu$g of type III pneumococcal polysaccharide (SSS-III) s.c. (gift from P. J. Baker, National Institute of Allergy and Infectious Diseases, National Institutes of Health). Ab titers were measured using Immulon-1 plates coated with 10 $\mu$g/ml *E. coli* LPS in PBS (pH 7.2) or 1 $\mu$g/ml SSS-III in 0.1 M HEPES (pH 3.5).

### *Statistics*

Differences in chemotaxis were determined using two-tailed *t* testing. Differences in Ab titers were determined using the two-tailed *t* tests on the geometric means of the reciprocals of the endpoint titers. The criterion for statistical significance was $p < 0.05$.

## Results

### *rMuMIG is a chemotactic factor for mouse T cells*

To characterize the function of Mig in mice and to understand its roles in mouse models of disease, we tested its activity as a chemotactic factor for mouse leukocytes. rMuMig had no chemotactic activity for polymorphonuclear leukocytes or for macrophages isolated from thioglycolate-induced peritoneal exudates, although these cells responded well to fMLP or recombinant human macrophage-inflammatory protein (MIP)-1$\alpha$ (CCL3), respectively; these cells also failed to respond to another murine CXCR3 ligand, recombinant cytokine-responsive gene (CRG)-2/IP-10 (data not shown). Responses of mouse $CD4^+$ and $CD8^+$ T cells to rMuMig were determined using splenocytes that either were freshly isolated or had been activated in vitro for 3 or 4 days using plate-bound anti-CD3. For the freshly isolated cells, we also stained for CD44 and CD62L to quantify naive and memory subsets. As shown in Fig. 1*A*, both $CD4^+$ and $CD8^+$ T cells, either freshly isolated or after activation in vitro, showed specific migration to rMuMig. Analysis of the freshly isolated cells that migrated to rMuMig using stains for CD44 and CD62L revealed that responses were found only in the memory, and not in the naive, subsets (Fig. 1*B*). As shown in Fig. 1*A*, the activated cells usually demonstrated more

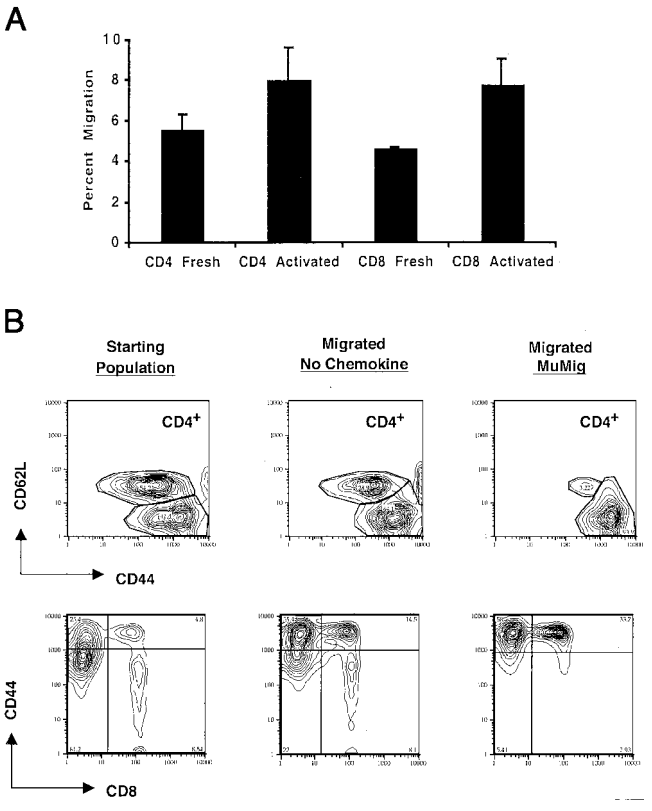


**FIGURE 1.** rMuMig is a chemotactic factor for mouse T cells. *A*, Splenocytes from C57BL/6 mice were used for chemotaxis assays either immediately after isolation (Fresh) or after activation with anti-CD3 for 4 days (Activated). Chemotaxis was measured using Transwell plates and $10^6$ cells/well. After 3 h at 37°C, cells from multiple bottom wells were pooled, counted, and stained for expression of CD4 and CD8. Data are expressed as the percentages of input $CD4^+$ or $CD8^+$ T cells migrating to the lower wells containing 1000 ng/ml rMuMig minus the percentages of cells migrating to lower wells containing medium alone. Data represent means and SEM of two experiments. Differences among these populations of cells were not statistically significant. *B*, Cells from the starting population of freshly isolated splenocytes or cells migrating to the lower chambers in the absence or presence of 1000 ng/ml rMuMig were stained for CD4 (Cy5-PE), CD44 (PE), and CD62L (FITC) or CD8 (FITC) and CD44 (Cy5-PE). Percentages of cells are indicated within the designated regions. Three additional experiments also showed that only memory cells migrated to rMuMig.

rMuMig-induced migration as compared with the freshly isolated cells, although the differences were not dramatic.

### *CXCR3 is expressed on mouse T cells*

Because mouse T cells responded to rMuMig we sought to analyze the expression of the mouse analog of human CXCR3, the only known human receptor for Mig, on these cells. Antiserum was raised against a carrier-conjugated peptide corresponding to aa 2–18 of the MuCXCR3 sequence. Anti-MuCXCR3 Abs were affinity-purified using the immunizing peptide and the Abs were shown to stain MuCXCR3 specifically by using transfected cells and by blocking staining with the immunizing peptide (see *Materials and Methods*; data not shown). Using these Abs, we found that a subset of total $CD8^+$ T cells showed staining that was blocked using the MuCXCR3 peptide (Fig. 2*A*). For freshly isolated total $CD4^+$ T cells there was also a suggestion of a $MuCXCR3^+$subset, but this was less clear. On 4-day activated T cells, specific staining for MuCXCR3 could be seen on both $CD4^+$ and $CD8^+$ T cells. For all cells, there was no staining seen with nonimmune rabbit IgG that could be blocked with the MuCXCR3 peptide (data not shown). We analyzed further the freshly isolated cells using CD44 and found that MuCXCR3 expression was limited to the $CD44^{bright}$, i.e., memory subsets (Fig. 2*B*), of both $CD4^+$ and $CD8^+$ cells, although there were higher numbers of the latter as compared with the former. The restricted expression of MuCXCR3 on memory cells is consistent with the results of the chemotaxis assays. There was a suggestion (Fig. 2*A*) that, while activation of $CD8^+$ T cells led to up-regulation of MuCXCR3 on the majority of cells, the level of MuCXCR3 might in fact have been reduced on the cells that were initially $MuCXCR3^+$. Freshly isolated $MuCXCR3^+CD8^+$ and $MuCXCR3^-CD8^+$ T cells were purified by cell sorting, activated in vitro, and stained for MuCXCR3. As shown in Fig. 2*C*, MuCXCR3 was induced on the population that was initially negative, whereas levels fell, but remained positive, on the (memory) $CD8^+$ T cells that were initially $MuCXCR3^+$.

### *Production of* $mig^{-/-}$ *mice*

To analyze the roles for MuMig in vivo, we produced mice with targeted disruption and partial deletion of the *mig* gene as shown in Fig. 3. Homologous recombination between the targeting DNA and the *mumig* gene was predicted to result in a deletion of 1458 bp of the *mumig* gene, including 104 bp of exon 2 and 1354 bp of the second intron, and insertion of the PGK/*neo* gene cassette containing multiple *Pst*I sites. An mRNA transcribed from the deleted/interrupted gene was predicted to encode the MuMig signal peptide followed by seven amino-terminal amino acids before reaching a stop codon. Moreover, the second exon sequence deleted in the recombinant allele contains three of the four cysteines conserved among the CXC and CC chemokines. Fig. 3 shows data from mice derived from two successfully targeted ES cells, clones 17 and 63. In addition to the results shown in Fig. 3, analysis of targeted DNAs revealed that the structure of the targeted allele was as predicted on both the 5′ and 3′ sides of the inserted DNA. Southern blot analysis using a probe for *crg-2/IP-10*, a gene within 100 kb of the *mumig* gene (H.-H. Lee and J. M. Farber, unpublished observations), showed the single wild-type band of >12 kb, suggesting that this neighboring locus was intact in the recombinants (data not shown).

The $mig^{-/-}$ and $mig^{+/+}$ $(129/Sv \times C57BL/6)F_2$ mice were analyzed for the expression of Mig mRNA and protein in tissues taken from mice that had been injected with rMuIFN-γ or from control-injected mice. As shown in Fig. 3*C*, Northern blot analysis using a probe prepared from the second exon of the *mumig* gene revealed induction in spleens of $mig^{+/+}$ mice injected with rMuIFN-γ but no signal in the $mig^{-/-}$ mice. Western blot analysis of liver microsomes revealed that no Mig protein was produced in response to rMuIFN-γ in the $mig^{-/-}$ mice (Fig. 3*D*). For the experiments shown below, $mig^{-/-}$ mice were used in both the $(129/Sv \times C57BL/6)F_2$ background and after backcrossing into C57BL/6 for six generations.

### $mig^{-/-}$ *mice have an abnormality in Ab production*

The $mig^{-/-}$ mice were born from $mig^{-/+}$ parents with expected frequencies and had no obvious abnormalities. Microscopic examination of H&E-stained tissues, including among them lymph nodes, spleen, and Peyer's patches, showed no differences in histology between $mig^{-/-}$ and $mig^{+/+}$ mice. Likewise, the $mig^{-/-}$ and $mig^{+/+}$ mice showed no differences in peripheral leukocyte and differential counts or in constituent populations of cells in thymus ($CD4^-CD8^-$, $CD4^+CD8^+$, and single-positive thymocytes), spleen ($CD4^+$ and $CD8^+$ T cells, B cells, macrophages, and NK cells), or peritoneum (B-1 B cells) as determined by flow

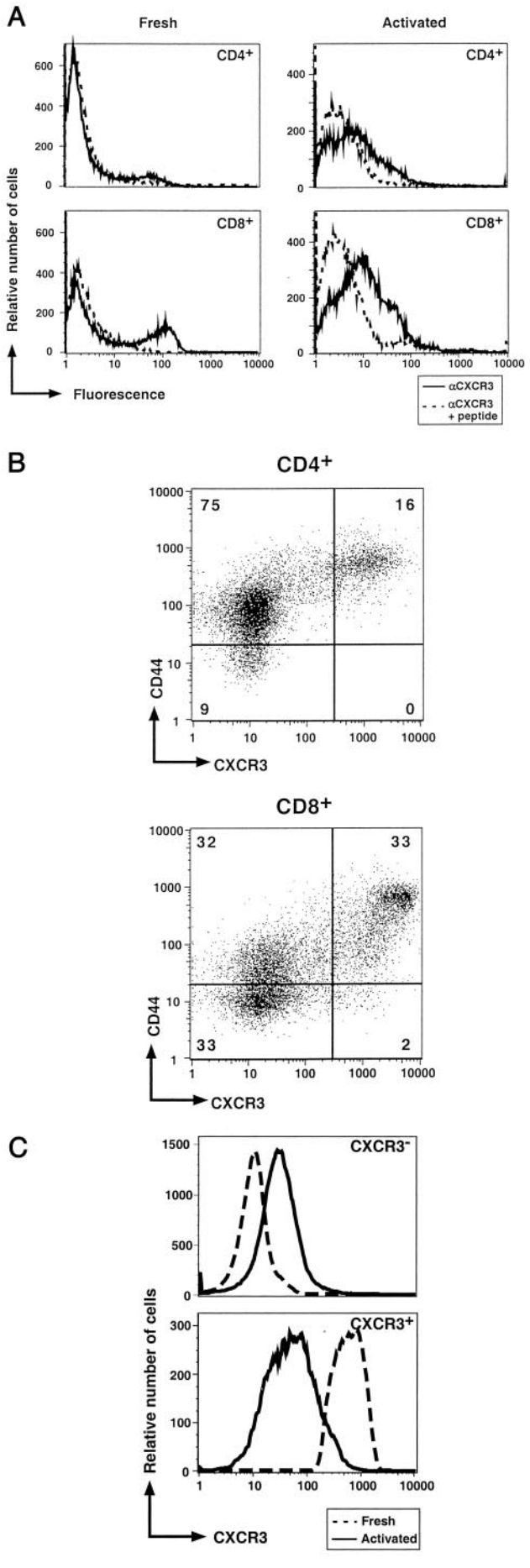


cytometry (data not shown). Because the expression of *mumig* in vivo is highly dependent on IFN-γ, we tested the $mig^{-/-}$ mice in models of host defense where IFN-γ plays a critical role. We found no significant differences in mortality between $mig^{-/-}$ mice and $mig^{+/+}$ mice infected with the following pathogens: *Listeria monocytogenes* (EGD strain, acute primary infection or after lethal challenge of surviving mice); *Salmonella typhimurium* (primary infection); *F. tularensis* LVS (acute primary infection or after lethal challenge of mice that survived primary sublethal infections); *Mycobacterium avium* (primary infection); *Toxoplasma gondii* (acute primary infection with ME-49 strain or immunization with strain TS-4 P1 followed by challenge with strain R.H.); vaccinia virus (primary infection); ectromelia virus (primary infection); hsv type 1 (immunization with KOS strain followed by challenge with McKrae strain); *Histoplasma capsulatum* (primary infection); and *Cryptococcus neoformans* (primary infection) (data not shown). Some of these models were analyzed in more detail. For example, we performed histological examination of liver inflammation after infection with *L. monocytogenes* or *T. gondii*; counted colonies of *L. monocytogenes* from spleens of infected mice; counted brain cysts in mice infected with *T. gondii*; analyzed peritoneal exudates after infection with *T. gondii* or splenocytes during the course of infection with *M. avium* by flow cytometry; and measured footpad swelling after inoculation with ectromelia virus. These analyses also failed to reveal significant and reproducible differences between the $mig^{-/-}$ and $mig^{+/+}$ mice (data not shown).

However, during analysis of responses to primary infections with the Gram-negative intracellular bacterium *F. tularensis* LVS we found that the $mig^{-/-}$ mice produced lower titers of Abs against the bacterium as compared with the $mig^{+/+}$ mice. The titers of anti-*Francisella* total IgG and the major isotype produced against the organism, $IgG_{2a/c}$ (37), were reduced in the $mig^{-/-}$ mice (Fig. 4). Diminished anti-*F. tularensis* LVS total IgG and/or $IgG_{2a/c}$ titers were found in the $mig^{-/-}$ vs $mig^{+/+}$ mice in each of six experiments using $(129/Sv \times C57BL/6)F_2$ or backcrossed mice using a range of sublethal doses of organisms (see Fig. 4). In two experiments in the 129/Sv background done with different doses of organisms, mean titers for IgG2a were also lower in the $mig^{-/-}$ mice, but the differences were not statistically significant (data not shown). No reproducible differences were found for anti-

**FIGURE 2.** Mouse T cells express CXCR3. *A*, Expression on fresh and activated $CD4^+$ and $CD8^+$ T cells. Splenocytes from C57BL/6 mice, either freshly isolated or after activation with anti-CD3 for 4 days, were stained for CD4 (allophycocyanin) and CD8 (FITC) and with rabbit anti-MuCXCR3 that had been preincubated with or without the MuCXCR3 immunizing (blocking) peptide. Cell-bound rabbit IgG was detected using biotinylated goat anti-rabbit Ab and streptavidin-PE. Fresh and activated $CD4^+$ and $CD8^+$ T cells are displayed separately as indicated. Solid lines represent staining without blocking peptide; dashed lines represent staining with blocking peptide. No peptide-inhibitable staining was seen using control rabbit IgG (data not shown). *B*, Expression on $CD4^+$ and $CD8^+$ T cell subsets. Freshly isolated splenocytes were stained for CD4 (allophycocyanin), CXCR3 (PE), and CD44 (FITC) or CD8 (allophycocyanin), CXCR3 (PE), and CD44 (FITC). Horizontal and vertical lines were drawn based on staining with an isotype control for CD44 (rat IgG2b conjugated to FITC) and with anti-MuCXCR3 in the presence of blocking peptide, respectively. The numbers in the quadrants represent the percentage of $CD4^+$ or $CD8^+$ T cells within each population. *C*, Effect of activation on expression on $CD8^+$ T cell subsets. $CD8^+$ T cells were sorted into $CD8^+CXCR3^-$ and $CD8^+CXCR3^+$ populations before activation with anti-CD3 and anti-CD28 for 4 days. CXCR3 (PE) staining of freshly isolated and activated sorted cells are shown using dashed lines and solid lines, respectively. Blocking peptide eliminated CXCR3 staining (data not shown). Data for each part are from one of at least two experiments that gave similar results.

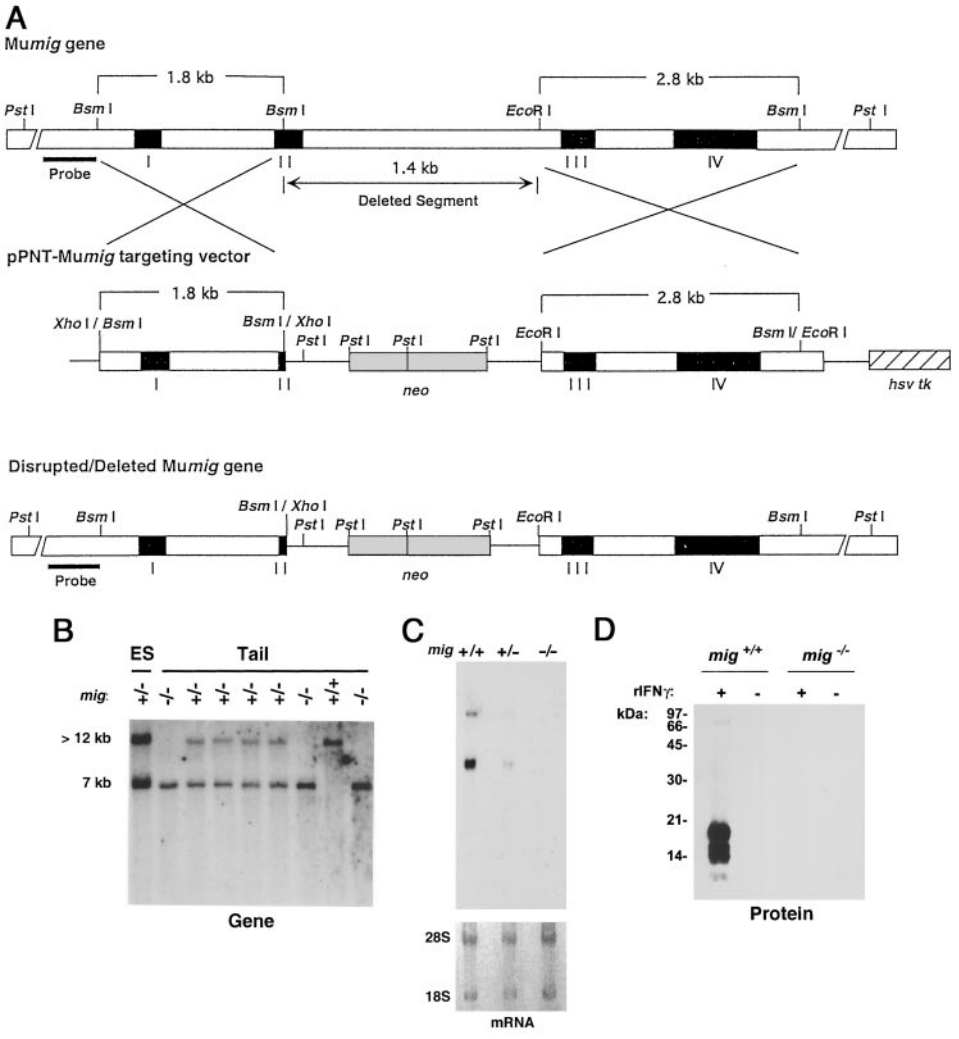


**FIGURE 3.** Disruption/deletion of the *mig* gene in mice. *A*, Targeting strategy. Schematic representations of the *mumig* gene, the pPNT-*mumig* DNA used for gene targeting, and the predicted disrupted/deleted gene are shown in the *upper*, *middle*, and *lower lines*, respectively. The *mumig* gene is on a *Pst*I fragment of >12 kb. The gene's four exons are shown as filled bars. The 5′ 1.8-kb and 3′ 2.8-kb restriction fragments inserted into the targeting DNA are indicated, as are the 1.4-kb fragment containing most of the second exon and intron that are predicted to be deleted in the targeted gene, and the probe that is 5′ to the targeting fragments and that was used to screen for homologous recombination. *Pst*I digestion of the targeted allele and hybridization to the 5′ probe was predicted to yield a band of ~6.9 kb. As shown on the *bottom line*, homologous recombination was expected to result in deletion of 1458 bp, including 104 bp of exon 2 and 1354 bp of the second intron, and insertion of the PGK/*neo* gene at this site. *B*, Genotypes of ES cell clone 17 and a single litter of mice from crossing (129/Sv × C57BL/6)$F_1$ parents heterozygous for the disrupted/deleted *mig* allele. DNAs from ES cells and from tail snippings of a litter of mice were digested with *Pst*I and hybridized with radiolabeled 5′ probe as indicated in *A*. The recombined *mig* allele yielded the predicted fragment of ~7 kb as indicated. The *mig* genotypes are indicated *above* the lanes: +/−, heterozygous; +/+, homozygous wild-type; −/−, homozygous knockout. *C*, $mig^{-/-}$ mice do not express Mig mRNA in spleen after injection with rMuIFN-γ. $mig^{+/+}$, $mig^{+/-}$, and $mig^{-/-}$ mice from line 63 were injected with 25,000 U rMuIFN-γ at 0 and 12 h and spleens were harvested at 24 h for preparation of RNA. Twenty micrograms of total RNA was loaded and hybridized to a radiolabeled probe containing sequences from the second exon of the *mumig* gene. The major species of MuMig mRNAs have mobilities of ~1.6 and 3 kb. Genotypes are indicated *above* the lanes. A photograph of the gel stained with ethidium bromide before transfer shows the ribosomal bands, demonstrating equal loading of total RNA per lane. An experiment using mice derived from ES cell line 17 gave similar results. *D*, $mig^{-/-}$ mice do not express Mig protein. $mig^{-/-}$ and $mig^{+/+}$ (129/Sv × C57BL/6)$F_2$ littermates from line 17 were injected with rMuIFN-γ or with carrier alone at 0 and 12 h before harvesting organs at 24 h. Livers were homogenized and microsomal pellets were prepared to enrich for secreted proteins. Microsomal samples containing 100 μg of protein were separated in a 15% acrylamide gel and electrotransferred to nitrocellulose. Each lane contained equal amounts of protein as visualized by staining with amido black (data not shown). The blot was probed with affinity-purified anti-MuMig rabbit Ig and rabbit Ab was detected using HRP-conjugated goat anti-rabbit IgG and a chemiluminescent substrate. Genotypes, the fractions analyzed, and injection with rMuIFN-γ (+) or carrier alone (−) are indicated *above* the lanes. MuMig runs as expected as multiple IFN-γ-inducible species below the 21-kDa marker. Two additional experiments analyzing mice derived from ES cell clone 17 and one experiment analyzing mice derived from ES cell clone 63 gave similar results.

*Francisella* LVS titers of IgM and of IgG1, IgG2b, and IgG3 for the $mig^{-/-}$ vs the $mig^{+/+}$ mice (data not shown). Bacterial clearance was comparable in the $mig^{-/-}$ and $mig^{+/+}$ mice in that no live organisms could be recovered from the spleens of either $mig^{-/-}$ or $mig^{+/+}$ mice 3 wk after infection. In addition, at 3 wk after infection, few small germinal centers could be seen in the spleens of both $mig^{-/-}$ and $mig^{+/+}$ mice by staining with peanut agglutinin (data not shown).

To determine whether the $mig^{-/-}$ mice responded abnormally to Ags not introduced by live infection, we analyzed responses of $mig^{-/-}$ and $mig^{+/+}$ mice to immunizations with the T cell-dependent Ag TNP-KLH and with the T cell-independent Ags LPS and SSS-III.

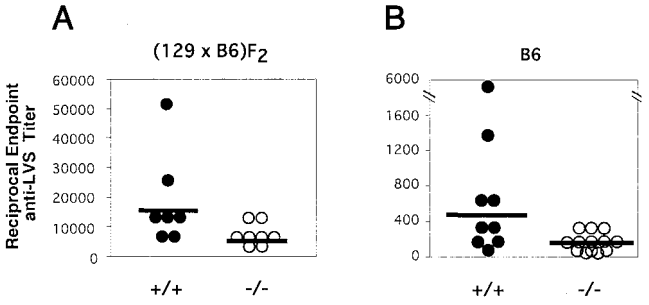


**FIGURE 4.** *mig*$^{-/-}$ mice produce lower titers of Ab against *F. tularensis* LVS. Two representative experiments are shown. Strain genotypes are indicated *above* the plots and *mig* genotypes are indicated *below*. Each circle represents an individual mouse; ● represents *mig*$^{+/+}$ mice and ○ represents *mig*$^{-/-}$ mice. Horizontal bars represent antilogarithms of geometric means. *A*, Serum total IgG against *F. tularensis* LVS was measured by ELISA 6 wk after i.d. infection of (129/Sv × C57BL/6)$F_2$ mice with $10^7$ organisms. The range of titers was 1/3,200–1/12,800 for the *mig*$^{-/-}$ mice and 1/6,400–1/51,200 for the *mig*$^{+/+}$ mice, and the mean endpoint titers were 1/4,935 for *mig*$^{-/-}$ mice and 1/15,596 for *mig*$^{+/+}$ mice, which are significantly different ($p < 0.04$). Two additional experiments using pooled sera also showed diminished anti-*F. tularensis* LVS IgG in the *mig*$^{-/-}$ mice. *B*, Serum $IgG_{2a/c}$ against *F. tularensis* LVS was measured by ELISA 3 wk after i.d. infection with $10^4$ organisms of *mig*$^{-/-}$ mice derived after backcrossing for six generations into the C57BL/6 strain vs C57BL/6 wild-type mice. The range of titers was 1/40–1/320 for the *mig*$^{-/-}$ mice and 1/80–1/5120 for the *mig*$^{+/+}$ mice, and the mean endpoint titers were 1/128 for *mig*$^{-/-}$ mice and 1/436 for *mig*$^{+/+}$ mice, which are significantly different ($p < 0.03$). A total of five experiments using (129/Sv × C57BL/6)$F_2$ or backcrossed mice showed diminished anti-*F. tularensis* LVS $IgG_{2a/c}$ titers in the *mig*$^{-/-}$ vs *mig*$^{+/+}$ mice.

No reproducible differences were seen in titers of IgG isotypes against TNP-KLH or in titers of total IgG against LPS (data not shown). Although in a limited number of experiments we found lower titers of IgM against TNP-KLH (by approximately one-half) at wk 1 in the *mig*$^{-/-}$ vs *mig*$^{+/+}$ mice, the difference was gone by wk 2, and no differences were seen in the titers of IgM against LPS or SSS-III (data not shown). Similarly, no differences were seen in pathogen-specific $IgG_{2a/c}$ titers between the two groups of mice measured during the first month of infection with *L. monocytogenes* or *T. gondii* (data not shown).

### *Activated B cells respond to rMuMIG and express CXCR3*

Although the diminished anti-*Francisella* LVS titers in the *mig*$^{-/-}$ mice could reflect the effects of MuMig on T cells or other non-B cells, we investigated the possibility that MuMig might target B cells directly. Although rMuMig had no chemotactic activity on freshly isolated mouse splenic B cells, B cells activated through Ag receptor and CD40 plus IL-4 showed dose-dependent migration to rMuMig (Fig. 5*A*). Dose-dependent responses to rMuMig of activated, but not resting, B cells were also seen using a flow cytometry-based calcium flux assay as shown in Fig. 5*B*. A time course revealed that acquiring responses to rMuMig required at least 4 days of activation of the B cells in vitro (data not shown).

We presumed that mouse B cell responses to rMuMig were mediated through CXCR3. In support of this presumption, rHuI-TAC (Fig. 5*B*) and rCRG-2/IP-10 (data not shown) also produced calcium fluxes in the activated $B220^+$ cells. Consistent with the data on chemokine-induced signals, activated but not resting B cells showed specific surface staining for CXCR3 that was blocked using the immunizing peptide (Fig. 6*A*) and Northern blotting revealed induction of CXCR3 mRNA after B cell activation (Fig. 6*B*).

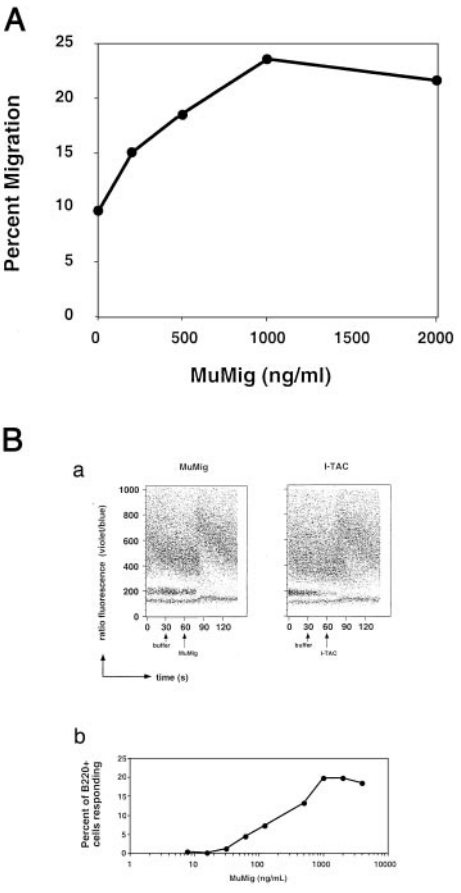


**FIGURE 5.** Activated B cells respond to CXCR3 ligands. *A*, Activated B cells migrate to MuMig. Single-cell suspensions from spleens of TCR$\beta^-\delta^-$ C57BL/6 mice were activated for 5 days with anti-IgM, IL-4, and CD40L. Chemotaxis was measured using a 96-well chemotaxis chamber, $10^5$ cells/well, and concentrations of rMuMig in the lower wells as shown. After 3 h at 37°C, cells from multiple bottom wells were pooled, counted, stained for B220, and compared with the starting population to determine the percentages of B cells migrating. Freshly isolated B cells did not migrate toward rMuMig and no net migration of activated B cells was seen when 1000 ng/ml rMuMig was put in both upper and lower wells (data not shown). A second experiment gave similar results. *B*, Activated B cells flux calcium in response to CXCR3 ligands. Single-cell suspensions from spleens of TCR$\beta^-\delta^-$ C57BL/6 mice were activated for 5 days with anti-IgM, IL-4, and CD40L before being loaded with indo-1, stained for B220, and used for calcium flux assays as described (8). *Ba*, In these scattergrams, the *y*-axes show channel numbers that reflect the fluorescence ratio of emissions at 390/530 nm of the calcium probe indo-1. For each assay, buffer was added at 30 s and rMuMig or rHuI-TAC was added as indicated at 60 s to a final concentration of 2000 ng/ml. Data are shown only for $B220^+$ cells. Freshly isolated B cells did not show a calcium flux in response to these ligands (data not shown). Data are from one of three experiments that gave similar results. *Bb*, Experiments were done as in *A*. A threshold value of ratio fluorescence was determined that separated the lower 95% from the highest 5% of cells following injection of buffer alone. The percentage of B cells rising above the threshold was determined at each concentration of rMuMig as described in *Materials and Methods* and in Ref. 8. The percentage value with buffer alone (5%) was subtracted from the values following rMuMig to obtain the percentage of responding cells.

### *Splenic dendritic cells express high levels of MuMig mRNA*

The data on B cells, together with the other data presented above, suggested that MuMig and CXCR3 might be involved not only in mediating trafficking to sites of peripheral inflammation but also in optimizing cell recruitment or cell-cell interactions within lymphoid organs. Therefore, we analyzed the expression of MuMig

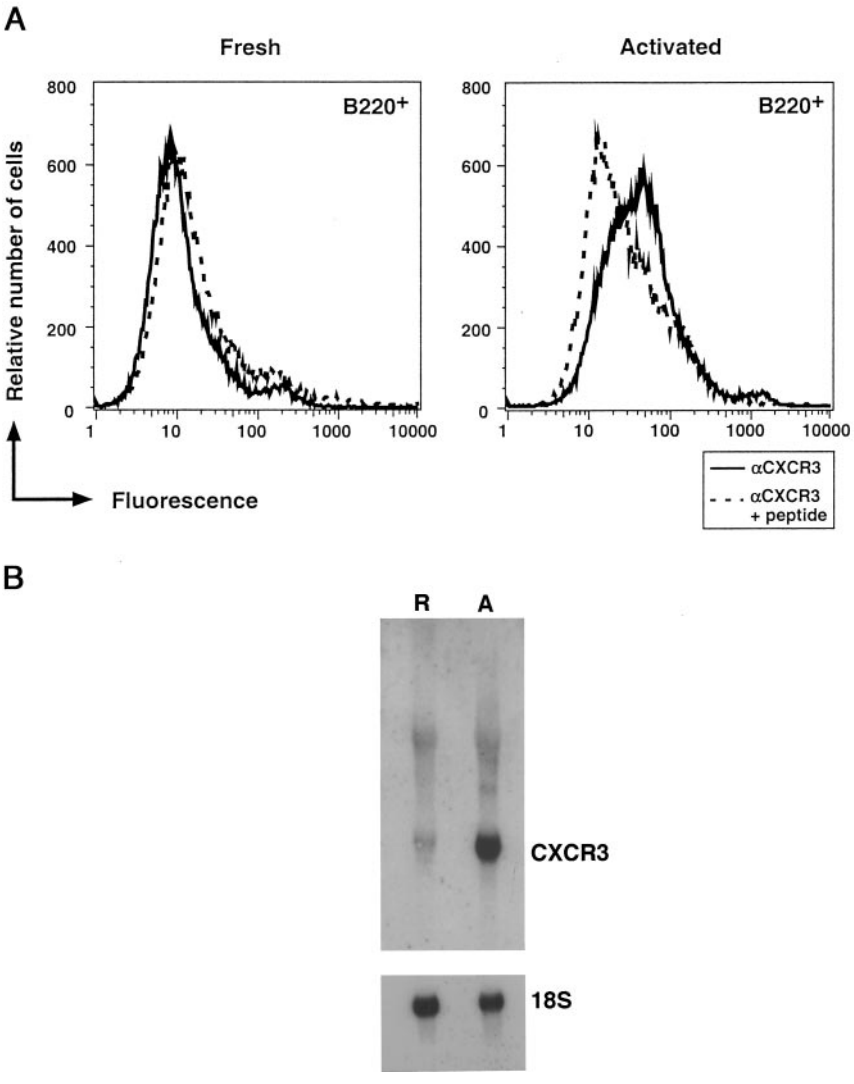


**FIGURE 6.** Activated mouse B cells express CXCR3. *A*, Activation induces surface expression of MuCXCR3. Cells purified from spleens of TCR$\beta^{-}\delta^{-}$ C57BL/6 mice were stained for B220, and with rabbit anti-MuCXCR3 that had been preincubated with or without the MuCXCR3 immunizing peptide. Cell-bound rabbit IgG was detected using biotinylated goat anti-rabbit Ab and streptavidin-PE. Solid lines represent staining without blocking peptide; dashed lines represent staining with blocking peptide. Data are shown only for B220$^{+}$ cells. *Left panel*, Freshly isolated B cells. *Right panel*, B cells after 5 days of activation with anti-IgM, rIL-4, and CD40L. No peptide-inhibitable staining was seen using control rabbit IgG (data not shown). Data are from one of two experiments that gave similar results. *B*, Activation induces the *Mu CXCR3* gene. Total RNA was prepared from splenic B cells from TCR$\beta^{-}\delta^{-}$ C57BL/6 mice, either immediately after isolation or after 6 days of activation with anti-IgM, rIL-4, and CD40L. Twenty micrograms of total RNA from resting (R) or activated (A) B cells was loaded per lane, fractionated in a 1.2% agarose/formaldehyde gel, transferred to reinforced nitrocellulose, and hybridized to a radiolabeled MuCXCR3 cDNA probe. The image was obtained using a PhosphorImager (Molecular Devices, Sunnyvale, CA). The MuCXCR3 mRNA ran just below the 18S ribosomal RNA. A radiolabeled oligonucleotide probe for the 18S ribosomal RNA was hybridized to the blot to demonstrate equal loading as shown. Data are from one of two experiments that gave similar results.

mRNA by semiquantitative RT-PCR before and after treatment with rMuIFN-$\gamma$ in subpopulations of mouse splenocytes sorted by flow cytometry. For comparison, we used RNA prepared from the RAW 264.7 mouse macrophage cell line where the mRNA for MuMig is known to be highly induced (38). As shown in Fig. 7, significant levels of MuMig mRNA could be detected in freshly isolated CD8$\alpha^{-}$ and CD8$\alpha^{+}$ splenic dendritic cells, and these levels could be dramatically enhanced by treatment with rMuIFN-$\gamma$ in vitro. Some expression and induction by rMuIFN-$\gamma$ was found in B cells as well, with no effect after short-term activation through surface IgM. T cells expressed the lowest levels of MuMig mRNA, with some induction by rMuIFN-$\gamma$ or by anti-CD3 plus anti-CD28. This latter induction was dependent on IFN-$\gamma$ because it was not seen using T cells isolated from IFN-$\gamma$ knockout mice (data not shown).

## Discussion

Mig and its receptor, CXCR3, have been presumed to function in the recruitment of effector T cells to sites of peripheral inflammation, and the limited data to date directly addressing function in vivo support this presumption (17, 19–21, 28). Nonetheless, some data have suggested a broader role. These have shown expression of CXCR3 on human B cells, including a subset of B cells in peripheral blood (24) and on the transformed cells in some B cell malignancies (39, 40), and roles for CXCR3 in T cell activation (28) and in inhibiting endothelial cell proliferation (41). We have characterized the expression and activities on mouse cells for MuMig and MuCXCR3, and we have investigated roles for MuMig and MuCXCR3 in vivo using gene-targeted *mig*$^{-/-}$ mice.

We have shown that MuMig is a chemotactic factor for freshly isolated memory CD8$^{+}$ and CD4$^{+}$ T cells as well as for both cell types after activation. We found that the activity of MuMig correlated with the expression of MuCXCR3, which was confined to the memory subsets of CD4$^{+}$ and CD8$^{+}$ T cells, and which was up-regulated on naive T cells and on B cells after activation. The up-regulation of MuCXCR3 with T cell activation is similar to the data for the human CXCR3 (8, 22), although in humans, unlike what we found in mice, CXCR3 is expressed on naive CD8$^{+}$ T cells. Activation of mouse memory CD8$^{+}$ T cells led to a fall in receptor levels. These data are similar to what we have found for human CD8$^{+}$ T cells, where there is a transient reduction in CXCR3 levels after activation with anti-CD3 and anti-CD28 (R. L. Rabin and J. M. Farber, unpublished observation). The biological consequences of this down-regulation are unlikely to be profound, in that the activated CD8$^{+}$ memory T cells do not become MuCXCR3$^{-}$, and, based on the high level of expression of MuCXCR3 on the freshly isolated CD8$^{+}$ memory T cells, we can presume that once the effector/memory CD8$^{+}$ cells come to rest, levels of MuCXCR3 rise. As regards the MuCXCR3 ligand

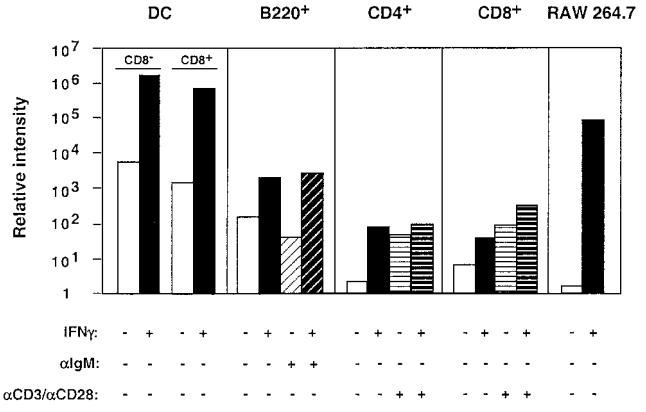


**FIGURE 7.** Expression of the *mumig* in splenic dendritic cells and lymphocytes. Semiquantitative RT-PCR analysis was performed as described (60) on total RNA from cells purified using a FACS and incubated for 18 h with (+) or without (−) 1000 U/ml rMuIFN-γ. CD8$\alpha^+$ and CD8$\alpha^-$ splenic dendritic cells were isolated and analyzed separately as noted. B cells were also incubated with (+) or without (−) 10 μg/ml anti-IgM and T cells with (+) or without (−) 10 μg/ml plate-bound anti-CD3 and 10 μg/ml soluble anti-CD28. Analysis was also done using RNA from the RAW 264.7 macrophage cell line incubated with (+) or without (−) 1000 U/ml rMuIFN-γ for 6 h to compare the signals in the primary cells with those in a cell line where the *mumig* gene is known to be highly inducible (38). Expression of *mumig* was normalized to the signals from hypoxanthine phosphoribosyltransferase and these values were then normalized to the lowest value obtained, which was from CD4$^+$ T cells isolated from IFN-γ$^{-/-}$ mice (data not shown), and which was set equal to 1. Data are from one of two experiments that gave similar results.

MuMig, we found that *mumig* was expressed not only by macrophages, as has been well documented (5), but also by the other APCs: MuMig mRNA could be induced to very high levels in splenic CD8$\alpha^-$ and CD8$\alpha^+$ dendritic cells and, to a lesser extent, in B cells. As far as we are aware, these are the first data showing expression of a CXCR3 ligand by bona fide populations of dendritic cells or by B cells.

Because of the preferential induction of *mig* by IFN-γ we tested the function of MuMig in models of host defense where IFN-γ is known to play a critical role. We found that MuMig was not essential for survival of primary infection and generation of a protective memory response after experimental infection with a variety of pathogens. We presume that at least part of the explanation for the lack of obvious deficits in host defense in the absence of MuMig was the result of the activities of the remaining MuCXCR3 ligands, CRG-2/IP-10 and MuI-TAC. Overlapping activities by other chemokine receptor/ligand groups might also be responsible.

Surprisingly, we found that *mig*$^{-/-}$ mice had diminished production of specific Abs against the bacterial pathogen *F. tularensis* LVS. Although the effect seen in the *mig*$^{-/-}$ mice in the 129/Sv × C57BL/6 or backcrossed C57BL/6 backgrounds was found consistently in repeated experiments and irrespective of the number of organisms injected, no differences in Ab responses were seen with pure protein or carbohydrate Ags, or with a limited number of other pathogens. Although we have no ready explanation for why our findings in the *mig*$^{-/-}$ mice have not been more general, possibilities include differences in the breadth, magnitudes, time courses, and sites of induction of MuMig and other chemokines by different Ags and pathogens. Nonetheless, defense against *F. tularensis* LVS depends on a host response where MuCXCR3 and its ligands would surely be anticipated to play a role, because an effective primary response is dependent on IFN-γ (42). Abs, while not essential for clearing infection, can provide anti-*Francisella* LVS benefit (37). Of additional interest, resistance to both early and late secondary challenge with *F. tularensis* LVS is dependent on B cells by a non-Ab-related mechanism (43).

The finding that MuMig has a role in maximizing Ab production is notable because it suggests that in some contexts Mig and CXCR3 may be important for optimizing T cell/APC/B cell interactions and thereby B cell function, presumably within lymphoid organs. This is a potential role for the CXCR3/CXCR3 ligand group that has not been previously appreciated. Both *mumig* (15) and *CRG-2/IP-10* (44) have been shown to be expressed within lymphoid organs and to be highly induced in response to infection or injection of rMuIFN-γ. For example, in the spleens of mice infected with *T. gondii*, in situ hybridization revealed expression of *mumig* and *CRG-2/IP-10* at the white-pulp/red-pulp margin and within the white pulp, where the signal came from CD11b$^+$ populations of cells, which should include macrophages and dendritic cells (15). Similarly, we have found that *humig* and *IP-10* are expressed by sorted populations of macrophages and dendritic cells isolated from human tonsils (R. L. Rabin and J. M. Farber, manuscript in preparation).

Given our current data on the expression and function of MuMig and MuCXCR3 in mouse cells and tissues we can speculate on the possible mechanisms underlying the effects of this ligand and receptor on Ab production. MuMig (and other CXCR3 ligands) and MuCXCR3 may be important for generating T cell help during a type 1 response. This could be due to a direct effect on T cell activation, as suggested from in vitro MLR experiments using cells from the MuCXCR3 knockout mice (28), or it could be a consequence of optimizing either the recruitment of activated T cells to dendritic cells and/or the quality T cell-dendritic cell interactions to support T cell expansion. A similar role has been suggested for another chemokine ligand/receptor pair, mouse macrophage-derived chemokine (CCL22) and CCR4 (45). Studies of human dendritic cells have also revealed prominent expression of macrophage-derived chemokine and thymus and activation-regulated chemokine (CCL17) (46, 47), which would be expected to attract Th2 cells selectively (48). From the data presented in this work and published previously (8, 26), expression of *mumig* by splenic dendritic cells would provide a parallel mechanism for recruitment of CD8$^+$ and Th1 cells, as well as recently activated T cells generally.

Our data also raise the possibility that the diminished Ab responses in the *mig*$^{-/-}$ mice were due wholly or in part to loss of a direct effect of MuMig on migration (or other responses) of activated B cells. In humans, CXCR3 has been found on the malignant cells in a high proportion of cases of both chronic lymphocytic leukemia and marginal zone lymphoma (39, 40), the former thought to represent a subset of follicular B cells and memory cells and the latter a subset of memory B cells that have undergone malignant transformation (49). One group has reported minimal chemotactic activity for IP-10 on nonmalignant human B cells (50), but others have failed to find such activity (40). A role for CXCR3 on normal B cells after activation has not been examined, and we found that induction of functional MuCXCR3 on mouse B cells in vitro required cellular activation. We have also found that CXCR3 is expressed on a subset of human tonsillar memory B cells but not on germinal center B cells (R. L. Rabin and J. M. Farber, unpublished observation). Together, these results suggest that CXCR3 may have a role on activated as well as memory B cells, although not on the majority of centroblasts/centrocytes that populate germinal centers.

Given these data, a possible direct role for CXCR3 in Ab responses would be in the recruitment of activated B cells and T cells

to Mig-producing dendritic cells to optimize B cell-T cell interactions. MuMig produced by B cells might also potentiate B cell-T cell interactions. Additionally, it is possible that CXCR3 and its ligands might be important for optimizing direct interactions between B cells and dendritic cells/macrophages. Dendritic cells have been shown to enhance B cell growth and differentiation and to boost Ig secretion (51). Of particular interest, the cell surface and secreted factor BLyS, which induces B cell proliferation and Ig secretion (52), is produced by IFN-γ-treated monocytes, macrophages, and dendritic cells (53), those cells expected to produce high levels of Mig and other CXCR3 ligands. Mig and other CXCR3 ligands may also influence Ab levels by affecting the migration of activated/memory B cells outside of lymphoid tissue, e.g., to peripheral sites where interactions with stromal cells can support optimal B lymphoblast survival and differentiation (54).

It has been proposed that inflammatory chemokines are unlikely to regulate trafficking within lymphoid organs (3), and certainly this view is reasonable if consideration is limited to migration within nonactivated tissue. In this case, compartment-specific chemokines such as secondary lymphoid tissue chemokine, EBV-induced receptor ligand chemokine, and B lymphocyte chemoattractant are the predominant factors in regulating T and B cell localization. Nonetheless, a lymph node responding to antigenic challenge adopts the functional characteristics typical of inflamed peripheral tissue (55). Our observations support the view that chemokine/ligand groups important for inflammation in peripheral tissue may also be playing a role in immune responses within lymphoid organs. Inflammatory chemokines other than Mig and IP-10 have also been found to be expressed within lymphoid organs (56). For example, MuMIP-1$\alpha$ and MuMIP-1$\beta$ (CCL4) have been demonstrated to be important in the recruitment of T cells to lymph nodes responding to Ag (57) and may be able to recruit memory T cells to Ag-activated B cells (58). In an activated lymphoid organ, inflammatory chemokines may be important not only in increasing the overall level of recruitment of lymphocytes but also in maximizing cell-cell interactions within compartments through chemotaxis and/or retention, and/or by enhancing intercellular adhesion through integrin activation. These activities do not preclude the possibility that inflammatory chemokines may have other direct effects on lymphocyte activation and differentiation (59). Together, our data demonstrate roles for MuMig and MuCXCR3 in B cell responses, extending our appreciation of the biological functions for this chemokine and receptor beyond that of mediating T cell trafficking to peripheral inflammatory sites and encouraging a broader perspective on the role of inflammatory chemokines in the immune response.

## Acknowledgments

We gratefully acknowledge Sylvia Montaner for providing MuCXCR3 in pCEFL, Hong Duc V. Dang and Diana Ngo for help in genotyping mice, and Ruth Swofford for help in cell sorting.

## References

1. Murphy, P. M., M. Baggiolini, I. F. Charo, C. A. Hebert, R. Horuk, K. Matsushima, L. H. Miller, J. J. Oppenheim, and C. A. Power. 2000. International union of pharmacology. XXII. Nomenclature for chemokine receptors. *Pharmacol. Rev. 52:145.*
2. Zlotnik, A., and O. Yoshie. 2000. Chemokines: a new classification system and their role in immunity. *Immunity 12:121.*
3. Moser, B., and P. Loetscher. 2001. Lymphocyte traffic control by chemokines. *Nat. Immunol. 2:123.*
4. Farber, J. M. 2000. Mig. In *Cytokine Reference.* J. J. Oppenheim and M. Feldmann, eds. Academic, London, p. 1111.
5. Farber, J. M. 1990. A macrophage mRNA selectively induced by γ-interferon encodes a member of the platelet factor 4 family of cytokines. *Proc. Natl. Acad. Sci. USA 87:5238.*
6. Farber, J. M. 1993. HuMig: a new human member of the chemokine family of cytokines. *Biochim. Biophys. Acta 192:223.*
7. Liao, F., R. L. Rabin, J. R. Yannelli, L. G. Koniaris, P. Vanguri, and J. M. Farber. 1995. Human Mig chemokine: biochemical and functional characterization. *J. Exp. Med. 182:1301.*
8. Rabin, R. L., M. K. Park, F. Liao, R. Swofford, D. Stephany, and J. M. Farber. 1999. Chemokine receptor responses on T cells are achieved through regulation of both receptor expression and signaling. *J. Immunol. 162:3840.*
9. Goebeler, M., A. Toksoy, U. Spandau, E. Engelhardt, E. B. Brocker, and R. Gillitzer. 1998. The C-X-C chemokine Mig is highly expressed in the papillae of psoriatic lesions. *J. Pathol. 184:89.*
10. Flier, J., D. M. Boorsma, D. P. Bruynzeel, P. J. Van Beek, T. J. Stoof, R. J. Scheper, R. Willemze, and C. P. Tensen. 1999. The CXCR3 activating chemokines IP-10, Mig, and IP-9 are expressed in allergic but not in irritant patch test reactions. *J. Invest. Dermatol. 113:574.*
11. Konig, A., V. Krenn, A. Toksoy, N. Gerhard, and R. Gillitzer. 2000. Mig, GROα and RANTES messenger RNA expression in lining layer, infiltrates and different leucocyte populations of synovial tissue from patients with rheumatoid arthritis, psoriatic arthritis and osteoarthritis. *Virchows Arch. 436:449.*
12. Simpson, J. E., J. Newcombe, M. L. Cuzner, and M. N. Woodroofe. 2000. Expression of the interferon-γ-inducible chemokines IP-10 and Mig and their receptor, CXCR3, in multiple sclerosis lesions. *Neuropathol. Appl. Neurobiol. 26: 133.*
13. Sorensen, T. L., M. Tani, J. Jensen, V. Pierce, C. Lucchinetti, V. A. Folcik, S. Qin, J. Rottman, F. Sellebjerg, R. M. Strieter, et al. 1999. Expression of specific chemokines and chemokine receptors in the central nervous system of multiple sclerosis patients. *J. Clin. Invest. 103:807.*
14. Yoong, K. F., S. C. Afford, R. Jones, P. Aujla, S. Qin, K. Price, S. G. Hubscher, and D. H. Adams. 1999. Expression and function of CXC and CC chemokines in human malignant liver tumors: a role for human monokine induced by γ-interferon in lymphocyte recruitment to hepatocellular carcinoma. *Hepatology 30: 100.*
15. Amichay, D., R. T. Gazzinelli, G. Karupiah, T. R. Moench, A. Sher, and J. M. Farber. 1996. Genes for chemokines MuMig and Crg-2 are induced in protozoan and viral infections in response to IFN-γ with patterns of tissue expression that suggest nonredundant roles in vivo. *J. Immunol. 157:4511.*
16. Mahalingam, S., J. M. Farber, and G. Karupiah. 1999. The interferon-inducible chemokines MuMig and Crg-2 exhibit antiviral activity in vivo. *J. Virol. 73:1479.*
17. Salazar-Mather, T. P., T. A. Hamilton, and C. A. Biron. 2000. A chemokine-to-cytokine-to-chemokine cascade critical in antiviral defense. *J. Clin. Invest. 105: 985.*
18. Sgadari, C., J. M. Farber, A. L. Angiolillo, F. Liao, J. Teruya-Feldstein, P. R. Burd, L. Yao, G. Gupta, C. Kanegane, and G. Tosato. 1997. Mig, the monokine induced by interferon-γ, promotes tumor necrosis in vivo. *Blood 89: 2635.*
19. Tannenbaum, C. S., R. Tubbs, D. Armstrong, J. H. Finke, R. M. Bukowski, and T. A. Hamilton. 1998. The CXC chemokines IP-10 and Mig are necessary for IL-12-mediated regression of the mouse RENCA tumor. *J. Immunol. 161:927.*
20. Koga, S., M. B. Auerbach, T. M. Engeman, A. C. Novick, H. Toma, and R. L. Fairchild. 1999. T cell infiltration into class II MHC-disparate allografts and acute rejection is dependent on the IFN-γ-induced chemokine Mig. *J. Immunol. 163:4878.*
21. Miura, M., K. Morita, H. Kobayashi, T. A. Hamilton, M. D. Burdick, R. M. Strieter, and R. L. Fairchild. 2001. Monokine induced by IFN-γ is a dominant factor directing T cells into murine cardiac allografts during acute rejection. *J. Immunol. 167:3494.*
22. Loetscher, M., B. Gerber, P. Loetscher, S. A. Jones, L. Piali, I. Clark-Lewis, M. Baggiolini, and B. Moser. 1996. Chemokine receptor specific for IP10 and mig: structure, function, and expression in activated T-lymphocytes. *J. Exp. Med. 184:963.*
23. Cole, K. E., C. A. Strick, T. J. Paradis, K. T. Ogborne, M. Loetscher, R. P. Gladue, W. Lin, J. G. Boyd, B. Moser, D. E. Wood, et al. 1998. Interferon-inducible T cell α chemoattractant (I-TAC): a novel non-ELR CXC chemokine with potent activity on activated T cells through selective high affinity binding to CXCR3. *J. Exp. Med. 187:2009.*
24. Qin, S., J. B. Rottman, P. Myers, N. Kassam, M. Weinblatt, M. Loetscher, A. E. Koch, B. Moser, and C. R. Mackay. 1998. The chemokine receptors CXCR3 and CCR5 mark subsets of T cells associated with certain inflammatory reactions. *J. Clin. Invest. 101:746.*
25. Farber, J. M., and B. Moser. 2000. CXCR3. In *Cytokine Reference.* J. J. Oppenheim and M. Feldmann, eds. Academic, London, p. 2003.
26. Sallusto, F., D. Lenig, C. R. Mackay, and A. Lanzavecchia. 1998. Flexible programs of chemokine receptor expression on human polarized T helper 1 and 2 lymphocytes. *J. Exp. Med. 187:875.*
27. Yamamoto, J., Y. Adachi, Y. Onoue, Y. S. Adachi, Y. Okabe, T. Itazawa, M. Toyoda, T. Seki, M. Morohashi, K. Matsushima, and T. Miyawaki. 2000. Differential expression of the chemokine receptors by the Th1- and Th2-type effector populations within circulating $CD4^+$ T cells. *J. Leukocyte Biol. 68:568.*
28. Hancock, W. W., B. Lu, W. Gao, V. Csizmadia, K. Faia, J. A. King, S. T. Smiley, M. Ling, N. P. Gerard, and C. Gerard. 2000. Requirement of the chemokine receptor CXCR3 for acute allograft rejection. *J. Exp. Med. 192:1515.*
29. Iwasaki, A., and B. L. Kelsall. 1999. Freshly isolated Peyer's patch, but not spleen, dendritic cells produce interleukin 10 and induce the differentiation of T helper type 2 cells. *J. Exp. Med. 190:229.*
30. Liao, F., A. K. Shirakawa, J. F. Foley, R. L. Rabin, and J. M. Farber. 2002. Human B cells become highly responsive to macrophage-inflammatory protein-3α/CC chemokine ligand-20 after cellular activation without changes in CCR6 expression or ligand binding. *J. Immunol. 168:4871.*

31. Soto, H., W. Wang, R. M. Strieter, N. G. Copeland, D. J. Gilbert, N. A. Jenkins, J. Hedrick, and A. Zlotnik. 1998. The CC chemokine 6Ckine binds the CXC chemokine receptor CXCR3. *Proc. Natl. Acad. Sci. USA 95:8205.*
32. Spencer, D. M., T. J. Wandless, S. L. Schreiber, and G. R. Crabtree. 1993. Controlling signal transduction with synthetic ligands. *Science 262:1019.*
33. Teramoto, H., O. A. Coso, H. Miyata, T. Igishi, T. Miki, and J. S. Gutkind. 1996. Signaling from the small GTP-binding proteins Rac1 and Cdc42 to the c-Jun N-terminal kinase/stress-activated protein kinase pathway: a role for mixed lineage kinase 3/protein-tyrosine kinase 1, a novel member of the mixed lineage kinase family. *J. Biol. Chem. 271:27225.*
34. Yu, C.-R., K. W. C. Peden, M. B. Zaitseva, H. Golding, and J. M. Farber. 2000. CCR9A and CCR9B: two receptors for the chemokine CCL25/TECK/Ck$\beta$-15 that differ in their sensitivities to ligand. *J. Immunol. 164:1293.*
35. Tybulewicz, V. L., C. E. Crawford, P. K. Jackson, R. T. Bronson, and R. C. Mulligan. 1991. Neonatal lethality and lymphopenia in mice with a homozygous disruption of the c-abl proto-oncogene. *Cell 65:1153.*
36. Cao, X., E. W. Shores, J. Hu-Li, M. R. Anver, B. L. Kelsall, S. M. Russell, J. Drago, M. Noguchi, A. Grinberg, E. T. Bloom, et al. 1995. Defective lymphoid development in mice lacking expression of the common cytokine receptor $\gamma$ chain. *Immunity 2:223.*
37. Rhinehart-Jones, T. R., A. H. Fortier, and K. L. Elkins. 1994. Transfer of immunity against lethal murine *Francisella* infection by specific antibody depends on host $\gamma$ interferon and T cells. *Infect. Immun. 62:3129.*
38. Farber, J. M. 1992. A collection of mRNA species that are inducible in the RAW 264.7 mouse macrophage cell line by $\gamma$ interferon and other agents. *Mol. Cell. Biol. 12:1535.*
39. Jones, D., R. J. Benjamin, A. Shahsafaei, and D. M. Dorfman. 2000. The chemokine receptor CXCR3 is expressed in a subset of B-cell lymphomas and is a marker of B-cell chronic lymphocytic leukemia. *Blood 95:627.*
40. Trentin, L., C. Agostini, M. Facco, F. Piazza, A. Perin, M. Siviero, C. Gurrieri, S. Galvan, F. Adami, R. Zambello, and G. Semenzato. 1999. The chemokine receptor CXCR3 is expressed on malignant B cells and mediates chemotaxis. *J. Clin. Invest. 104:115.*
41. Romagnani, P., F. Annunziato, L. Lasagni, E. Lazzeri, C. Beltrame, M. Francalanci, M. Uguccioni, G. Galli, L. Cosmi, L. Maurenzig, et al. 2001. Cell cycle-dependent expression of CXC chemokine receptor 3 by endothelial cells mediates angiostatic activity. *J. Clin. Invest. 107:53.*
42. Yee, D., T. R. Rhinehart-Jones, and K. L. Elkins. 1996. Loss of either $CD4^+$ or $CD8^+$ T cells does not affect the magnitude of protective immunity to an intracellular pathogen, *Francisella tularensis* strain LVS. *J. Immunol. 157:5042.*
43. Culkin, S. J., T. Rhinehart-Jones, and K. L. Elkins. 1997. A novel role for B cells in early protective immunity to an intracellular pathogen, *Francisella tularensis* strain LVS. *J. Immunol. 158:3277.*
44. Gattass, C. R., L. B. King, A. D. Luster, and J. D. Ashwell. 1994. Constitutive expression of interferon $\gamma$-inducible protein 10 in lymphoid organs and inducible expression in T cells and thymocytes. *J. Exp. Med. 179:1373.*
45. Tang, H. L., and J. G. Cyster. 1999. Chemokine up-regulation and activated T cell attraction by maturing dendritic cells. *Science 284:819.*
46. Hashimoto, S., T. Suzuki, H. Y. Dong, S. Nagai, N. Yamazaki, and K. Matsushima. 1999. Serial analysis of gene expression in human monocyte-derived dendritic cells. *Blood 94:845.*
47. Vissers, J. L., F. C. Hartgers, E. Lindhout, M. B. Teunissen, C. G. Figdor, and G. J. Adema. 2001. Quantitative analysis of chemokine expression by dendritic cell subsets in vitro and in vivo. *J. Leukocyte Biol. 69:785.*
48. Imai, T., M. Nagira, S. Takagi, M. Kakizaki, M. Nishimura, J. Wang, P. W. Gray, K. Matsushima, and O. Yoshie. 1999. Selective recruitment of CCR4-bearing Th2 cells toward antigen-presenting cells by the CC chemokines thymus and activation-regulated chemokine and macrophage-derived chemokine. *Int. Immunol. 11:81.*
49. Pascual, V., Y. J. Liu, and J. Banchereau. 1997. Normal human B cell subpopulations and their malignant counterparts. *Baillieres Clin. Haematol. 10:525.*
50. Nielsen, L. S., J. Frydenberg, M. Lind, M. Deleuran, K. Stengaard-Pedersen, and B. Deleuran. 1997. CD19-selected B lymphocytes synthesize, secrete and migrate in the presence of IL-8: TNF-$\alpha$ and $\gamma$IP-10 are also B lymphocyte migratory factors. *Cytokine 9:747.*
51. Dubois, B., B. Vanbervliet, J. Fayette, C. Massacrier, C. Van Kooten, F. Briere, J. Banchereau, and C. Caux. 1997. Dendritic cells enhance growth and differentiation of CD40-activated B lymphocytes. *J. Exp. Med. 185:941.*
52. Moore, P. A., O. Belvedere, A. Orr, K. Pieri, D. W. LaFleur, P. Feng, D. Soppet, M. Charters, R. Gentz, D. Parmelee, et al. 1999. BLyS: member of the tumor necrosis factor family and B lymphocyte stimulator. *Science 285:260.*
53. Nardelli, B., O. Belvedere, V. Roschke, P. A. Moore, H. S. Olsen, T. S. Migone, S. Sosnovtseva, J. A. Carrell, P. Feng, J. G. Giri, and D. M. Hilbert. 2001. Synthesis and release of B-lymphocyte stimulator from myeloid cells. *Blood 97:198.*
54. Shimaoka, Y., J. F. Attrep, T. Hirano, K. Ishihara, R. Suzuki, T. Toyosaki, T. Ochi, and P. E. Lipsky. 1998. Nurse-like cells from bone marrow and synovium of patients with rheumatoid arthritis promote survival and enhance function of human B cells. *J. Clin. Invest. 102:606.*
55. Mackay, C. R., W. Marston, and L. Dudler. 1992. Altered patterns of T cell migration through lymph nodes and skin following antigen challenge. *Eur. J. Immunol. 22:2205.*
56. Tedla, N., P. Palladinetti, D. Wakefield, and A. Lloyd. 1999. Abundant expression of chemokines in malignant and infective human lymphadenopathies. *Cytokine 11:531.*
57. Tedla, N., H. W. Wang, H. P. McNeil, N. Di Girolamo, T. Hampartzoumian, D. Wakefield, and A. Lloyd. 1998. Regulation of T lymphocyte trafficking into lymph nodes during an immune response by the chemokines macrophage inflammatory protein (MIP)-1$\alpha$ and MIP-1$\beta$. *J. Immunol. 161:5663.*
58. Krzysiek, R., E. A. Lefevre, W. Zou, A. Foussat, J. Bernard, A. Portier, P. Galanaud, and Y. Richard. 1999. Antigen receptor engagement selectively induces macrophage inflammatory protein-1$\alpha$ (MIP-1$\alpha$) and MIP-1$\beta$ chemokine production in human B cells. *J. Immunol. 162:4455.*
59. Luther, S. A., and J. G. Cyster. 2001. Chemokines as regulators of T cell differentiation. *Nat. Immunol. 2:102.*
60. Park, M. K., K. F. Hoffmann, A. W. Cheever, D. Amichay, T. A. Wynn, and J. M. Farber. 2001. Patterns of chemokine expression in models of *Schistosoma mansoni* inflammation and infection reveal relationships between type 1 and type 2 responses and chemokines in vivo. *Infect. Immun. 69:6755.*